

Research Article

An Experimental Study PVDF and PSF Hollow Fiber Membranes for Chemical Absorption Carbon Dioxide

Ehsan Kianfar 

Department of Chemical Engineering, Arak Branch, Islamic Azad University, Arak, Iran
Email: ehsan_kianfar2010@yahoo.com; e-kianfar94@iau-arak.ac.ir

Received: 27 July 2020 ; Revised: 8 September 2020 ; Accepted: 8 September 2020

Abstract: Poly(vinylidene fluoride) (PVDF) and Polysulfone (PSF) polymer solutions were made at a concentration of 18% by weight of the polymer as a non-soluble additive in polymer solution in 1-methyl-2-pyrrolidone (NMP) solvent. PVDF and PSF hollow fiber membranes were fabricated via the wet phase-inversion process. Fabricated membranes were characterized in terms of gas permeability, wetting resistance, water contact angle, and overall porosity. In order to study the structure of the membranes made, the scanning electron microscopy images of the model (TM3000, Hitachi, Japan) were used. The morphology study indicates that the PSF membrane shows an open cross-section structure with smaller pore sizes. However, the PVDF membrane illustrates a thick sponge-like structure. The fabricated PVDF membrane shows higher wetting resistance, surface porosity, water contact angle, and N_2 permeability. The performance of the produced membranes was examined for the absorption of carbon dioxide in a gas-liquid contactor membrane through the solution of Monoethanolamine (MEA). The results show that the CO_2 absorption flux of the PVDF hollow fiber membrane is higher than that of the PSF hollow fiber membrane. The maximum CO_2 absorption flux of 8.10×10^{-3} (mol·m⁻²·s⁻¹) at the liquid phase flow rate of 300 mL·min⁻¹ for PVDF hollow fiber membrane was achieved, and the maximum CO_2 absorption flux of 6.50×10^{-3} (mol·m⁻²·s⁻¹) at the liquid phase flow rate of 300 mL·min⁻¹ for the PSF hollow fiber membrane was obtained. It can be concluded that a porous hydrophobic hollow fiber membrane with high surface porosity and high gas permeability can be a productive alternative for CO_2 absorption through gas-liquid membrane contactors.

Keywords: hollow fiber membrane, gas-liquid contracting process, chemical absorption, Poly(vinylidene fluoride) (PVDF), Polysulfone (PSF)

1. Introduction

Global warming is mainly due to greenhouse gas emissions, the major part of which is carbon dioxide gas¹⁻³. Carbon capture and storage is one of several solutions recommended by the International Energy Agency to reduce the impact of human activities on the global climate. Using this technology may reduce carbon dioxide emissions by 14% to 17%⁴. The technologies currently used in the gas confectionery industry to absorb carbon dioxide gas are dependent on the absorption of carbon dioxide by amine-based chemical solvents. Monoethanolamine (MEA) is currently the most important industry-standard solvent for the carbon dioxide capture process⁵⁻⁶. Upon absorption of carbon dioxide gas, the carbon dioxide gas released. The minimum energy required to absorption 90% of carbon dioxide gas from a coal-

fired power plant is about 4-5% of the pure electricity produced by the same plant. Carbon dioxide gas absorption by monoethanolamide without compression is about 5 times the minimum energy required. The release of this gas in the air has increased the temperature of the planet. According to all the reasons for the improvement and economization of gas refining equipment, the removal of carbon dioxide from industrial streams and domestic use, and especially natural gas (down to mole%), is essential because of the huge reserves of this critical substance in the country⁷⁻⁹. Extensive methods for removing carbon dioxide by Absorption in alkane amine ammonium solutions are available with conventional equipment, tray towers, bubble towers, filled towers, and spray towers. The use of alkane amines allows us to rehydrate the liquid solvent by simply heating. Therefore, a carbon dioxide capture process involves two major absorption and stripping units¹⁰. This process has operational problems such as overcrowding, channelization, persistence, and fatigue¹¹⁻¹³. Today, these processes are known as a suitable alternative to the traditional gas absorption processes with an amine solution. Membrane processes have major benefits to absorption processes. Lower power consumption, lower operating costs, less initial installation and investment, no risk of fire and explosion, being very suitable and compatible with environmental laws, etc.¹⁴⁻¹⁷. The nerve fiber membrane collision system is one of the preferred methods to be considered by researchers¹⁸⁻²⁰. In this system, two-phase fluids collide with an appropriate membrane structure. For example, in a hollow fiber membrane, a common gas-liquid interface occurs at the mouth of the membrane pores²¹⁻²³. Current developments in the chemical industry and similar industries have led to increased process speed and reduced energy consumption throughout the process²⁴⁻²⁶. One of the most important processes in such industries is the separation of different materials. To perform industrial processes, raw material components must often be separated and the product obtained from these processes must be separated and purified. On the other hand, in most industries, taking into account environmental laws, the need for separation processes is more than ever before²⁷. In fact, as the separating processes and the related equipment are so large that in most industries, a large part of the cost of a product is related to the costs of separating and purifying the product²⁸. For this reason, finding a simpler separation method at a lower cost can be considered. In choosing an appropriate separation method, the efficiency of those methods, access to equipment, separation costs, cost of construction and energy costs should be fully evaluated, taking into account environmental issues and policy issues²⁹. Also, the separation targets must be specified in the process. In a separation process, different goals such as concentration, purification, separation, and displacement of the reaction balance can be considered. In this regard, membranes have been developed for the separation of various types of materials in solid, liquid, and gas states³⁰. One of the most important factors is the type of polymer used in membrane fabrication. Typically the polymer used to make the membrane is for use in the hydrophobic gas-liquid membrane contactor system to prevent the penetration of the Absorption liquid into the membrane pores. The penetration of the Absorption liquid into the pores of the membrane will block the pores and reduce the level of contact between the gas and the liquid. This increases the mass transfer resistance and reduces the gas absorption flux³¹⁻³⁶.

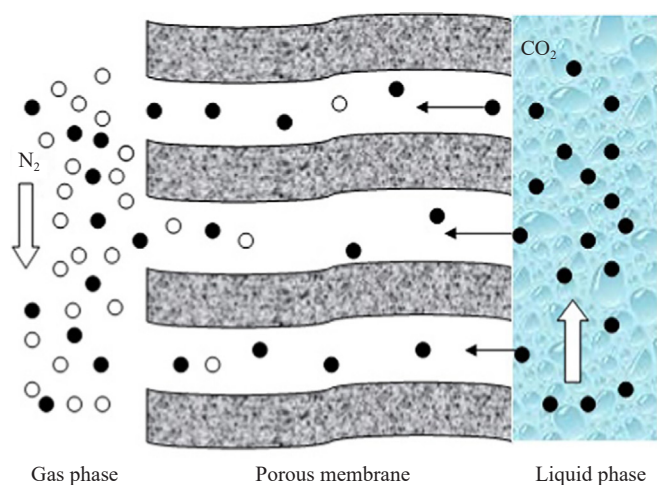


Figure 1. CO₂ absorption phase gas-liquid membrane contactors system²⁷

Table 1. Research findings on CO₂ absorption flux by other researchers

Membrane type	Liquid absorbent	CO ₂ absorption flux (mol·m ⁻² ·s ⁻¹)	Reference
HF PVDF	1 M MEA	8.0×10^{-3}	61
PTFE	5 M MEA	2.03×10^{-3}	62
PTFE	0.03 AMP	1.08×10^{-4}	63
PP	0.5 M MEA	4.4×10^{-4}	64
PVDF/triacetin	0.5 M NaOH	$(1-3.2) \times 10^{-3}$	65
PVDF, PTFE	2 M MEA	1.08×10^{-2}	66
PVDF	1 M MEA	7.2×10^{-4}	67
PSF	1 M MEA	3.9×10^{-3}	27

*HF PVDF–Hollow Fiber Poly(vinylidene fluoride); PTFE–Polytetrafluoroethylene; PP–Polypropylene; PSF–Polysulfone; MEA–Monoethanolamine; AMP–2-Amino-2-methyl-1-propanol

The penetration of water into the membrane pores reduces the contact surface between the gas and liquid and reduces the mass transfer rate. For this reason, in liquid-gas membrane contact systems, water-based polymers, such as PVDF, are commonly used. On the other hand, the structure and physical properties of the membrane, such as the diameter of the pores, total porosity, the critical pressure of water entering the pores, the angle of water contact with the membrane, also affect the membrane function. Therefore, it is necessary to study the performance of various polymers in the gas-liquid membrane contact system³⁷⁻⁴². The mechanism of CO₂ absorption is shown in Figure 1. Table 1 summarizes several findings of absorption performances that have been reported by various researchers for the past 10 years. Research objectives include the following:

- (1) Making a membrane of fiber between PSF and PVDF in a phase separation method.
- (2) Determine the profile and structure of the membranes made.
- (3) Using membranes made to Absorption carbon dioxide gas by a 1 molar monoethanolamide aqueous solution in a gas and liquid membrane contact system.

2. Materials and methods

2.1 Materials

PSF polymer Udel P-1700 (Solvay Advanced Polymers) and PVDF Polymer Commercial (Kynar® 740, Mn = 156,000) from Arkema Inc. The USA were used to make the nylon fiber membrane. 1-Methyl-2-Pyrrolidine (NMP > 99.5%) was purchased from Merck, which was used as a non-purified solvent. Monoethanolamide (99%) supplied by Sigma-Aldrich was used as a gas absorbent. Water was used as a coagulation bath in the process of making membranes^{1,43-45}.

2.2 Polymer solution preparation

18% by weight solutions of PSF and PVDF polymers were prepared in the diethylamide solvent. To make any kind of polymer solution, the specified amount of solvent was weighed and poured into a glass bottle. Then, the specific amount of each weighted polymer was gradually added to the solvent so that the polymer beads did not clump together⁴⁶⁻⁵⁰. The solutions were stirred using a mechanical stirrer to dissolve all the polymer grains in the solvent. After the polymer grains were completely dissolved in the solvent, the solutions were placed in ultrasonic for 1 hour to remove air bubbles in the polymer solutions. If there is an air bubble in the polymer solution, the bubble is formed on the surface of the bubble and the membrane is torn. The viscosity of the polymer solutions was also measured using a Cole Parmer viscometer, EW-98965-40, USA. The composition of the materials used to make the polymer solutions and

the viscosity of the solutions are shown in Table 2.

Table 2. Composition of the materials polymer solutions and the viscosity of the solutions

polymer solutions	Polymer (Wt. %)	NMP (Wt. %)
PSF	18	82
PVDF	18	82

2.3 *CO₂ Absorption experiment*

The carbon dioxide gas uptake flux was measured with a 1 M monoethanolamide solution in a gas-liquid membrane contact system. For this purpose, a set of mid-hollow fiber membranes containing 10 membranes was inserted in a stainless steel module as described in Table 3. Pure carbon dioxide gas using the pressure of the gas tank in the membrane conduit and the 1 M monoethanolamide solution as a liquid adsorbent by pumping into the module shell and discordantly. The gas flow rate was constant at 200 mL·min⁻¹ and the fluid flow intensity varied in the range of 50–300 mL·min⁻¹. The gas-phase pressure was set at 1 bar and the liquid phase pressure was 0.2 times higher than the gas phase pressure to prevent bubble formation in the liquid⁵¹⁻⁵³. Carbon dioxide concentration was measured in the output fluid of the module by the titration method. To titrate 10 ml of the output fluid from the module that absorbed carbon dioxide gas was poured into an Erlenmeyer and added 12 ml of 1 M sodium hydroxide (NaOH) solution to dissolve the dissolved carbon dioxide gas. Not in the solution, there is completely ionized. Then 5 ml of barium chloride solution (BaCl₂) was added to the solution. Then the obtained solution was shaken well until all the carbon dioxide dissolved in the solution (physically or chemically) deposit as barium carbonate (BaCO₃). The residual amount of sodium hydroxide in the solution was titrated with Hydrogen Chloride (HCl) and phenolphthalein was used as the reagent. The amount of hydrochloric acid used in this step is used to calculate the amount of carbon dioxide absorbed as a mole of carbon dioxide per mole of monoethanolamide. Before sampling for titration, the gas uptake test was performed in the gas-liquid membrane contactor system for 30 min to standardize the test conditions. The amount of HCl is used in this stage to calculate the amount of carbon dioxide Absorption by the moles of carbon dioxide (CO₂) to the number of moles of MEA. Before taking samples, all tests were performed for 30 minutes to achieve a steady state.

$$J_{\text{CO}_2} = \frac{Q_L \cdot M_{\text{CO}_2}}{V_{\text{sample}}} \times 1,000 \quad (1)$$

The total area of the membrane was considered as the surface liquid-gas contact deal for mass transfer, so the empirical amount of carbon dioxide flux J_{CO_2} ($\frac{\text{mol}}{\text{V}_{\text{sample}}}$) is calculated from the following relation:

$$M_{\text{CO}_2} \left(\frac{\text{mol}}{L} \right) = \frac{(N \cdot V)_{\text{HCl}}}{V_{\text{sample}}} \quad (2)$$

Where Q_L is Absorption flow rate (m³·s⁻¹), M_{CO_2} is the concentration of carbon dioxide in the Absorption solution (mol/L) and A_i is the collision surface between air-liquid (m²). Absorption membrane contactor-module output flow rate was measured by a liquid flow meter. Gas-liquid contact surface is measured based on Absorption flow on the pipe or the surface contact module. When the liquid Absorption flows on the shell side, the surface area is calculated using the following relation:

$$A_0 = n\pi d_i L \quad (3)$$

Where n is the number of fibers (in this study, 10), d_i is inner diameter of fibers, and (m) and L are effective fiber length. In this system, two-phase fluid system uses a membrane structure appropriate to collide. For example, the shared level of gas-liquid is created in the opening of membrane pore. Gas-liquid hollow fiber membrane contactor can be a promising alternative for the CO_2 absorption processes. In this system, the porous membrane acts as a fixed interface between the gas and liquid phases without dispersing one phase into another. The form of the pilot reactor is shown in Figure 2.

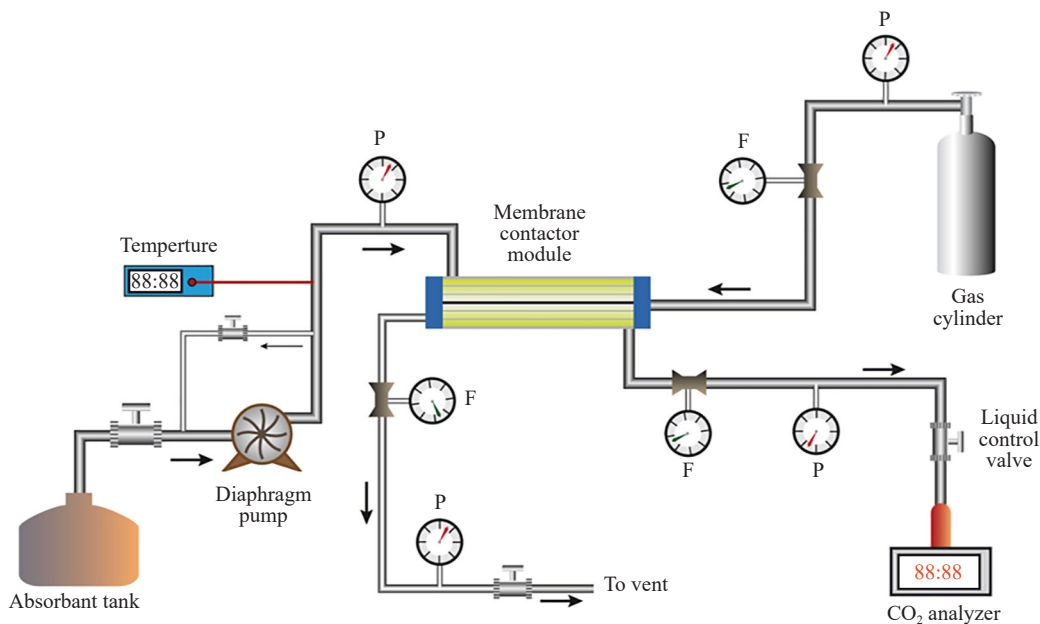


Figure 2. Absorption carbon dioxide system²⁷

Table 3. Properties of fabricated PSF and PVDF hollow fiber membranes

Dope extrusion rate ($\text{mL} \cdot \text{min}^{-1}$)	4.5
Bore composition (wt. %)	80/200 NMP/Water
Bore flow rate ($\text{mL} \cdot \text{min}^{-1}$)	1.55
external coagulant	Tap water
Air gap distance (cm)	0.0
the outer diameter of the inner spinner (mm)	0.55-1.2
Spinning dope temperature (°C)	25
External coagulant temperature (°C)	25
The inner diameter of the module (mm)	14
Length of the module (mm)	270
Output diameter fiber (mm)	0.70-0.90
Input diameter of fibers (mm)	0.45-0.50
The effective length of fiber (mm)	150
The number of fibers	10
Contact area	4,521 in

2.4 Fabrication and characterization of porous hollow fiber membranes

PVDF and PSF Polymer (PSF and PVDF Udel P-1700-Solvay Advance Polymer) for the building hollow fiber membranes: 1-methyl, 2-pyrrolidone (NMP > 99.5%) as a gross solvent and ethanol as non-solvent additives were purchased from Merck Company Germany. In all cases tap water was used as coagulation bath (spinning process). Monoethanolamine (MEA > 98%) was purchased from Sigma-Aldrich Co and used as the absorbent liquid. Table 2 and Table 3 show the Properties of fabricated PVDF and PSF hollow fiber membranes. dope was applied as an external coagulant for solidification of polymer solution resulting in formation of hollow fiber. After that the Spinneret hollow fiber was drowned into the water for three days to remove the ethanol and remaining NMP. Then it was naturally hung to be dried in environment temperature for one to two days.

3. Results and discussion

The cross-sectional and internal surface structure of the membranes made by scanning electron microscopy was investigated. Figures 3 and 4 show the cross-sectional and internal surfaces of the nylon fibers. The membranes have an external diameter of from 0.70 to 0.90 mm, the inner diameter is from 0.45 to 0.50 mm and the wall thickness is from 0.225 to 0.250 mm. Because all the membranes were made at the same rate of discharge of the polymer solution and the diffusion fluid flow rate, they were approximately equal in size. In general, the structure of the membrane depends on the rate of change in the phase of the polymer solution in the phase separation process. The change in the phase of the polymer solution depends on the viscosity of the polymer solution. A polymer solution with a viscosity has a faster phase change. The viscosity of the polymer solution affects the penetration rate of the coagulant to the membrane structure, so the less viscosity of the polymer solution results in a finger-shaped structure. The viscosity of polymer solutions is presented in Table 4. The cross-sectional images of the PVDF membrane indicate that a thick sponge layer is formed in the middle of the membrane that is surrounded by a low thickness finger structure on the inner and outer surfaces of the membrane. Due to the hydrophobicity of the polymer of PVDF, the phase separation process is slow during the construction of this membrane, which can be attributed to the formation of a thick sponge layer in this membrane. As shown in Figure 3 (a) and (b), the PSF membrane cross-section has a thick thumb structure near the outer surface of the membrane, with a low thickness foam structure near the inner surface of the membrane. According to Table 4, the viscosity of the solution of PSF is determined from the viscosity of the solution the less Poly(vinylidene fluoride) is due to the formation of the thickening of the fingers of this membrane. Due to the use of water (non-solvent) in the coagulation bath, the fingertip is formed at the outer surface of the PSF membrane because water as a non-solvent polymer separation rate accelerates the phase. From Figures 3 and 4 (c), it is understood that the use of high solvent concentration as Figures 3 and 4 (c) disintegrate slows down the phase separation process and forms an unclosed inner surface with an open structure with a finer porosity and is the same structure of the study for Polyvinyl dine Fluoride membranes using 90% by weight of solvent as a fluid⁵⁴⁻⁵⁶. Removal of the inner shell of the membrane could reduce the membrane's resistance to mass transfer in the gas absorption process.

Table 4. Viscosity polymer solutions

polymer solutions	Viscosity polymer solutions (cp at 25 °C)
PVDF	2,815.3
PSF	930.6

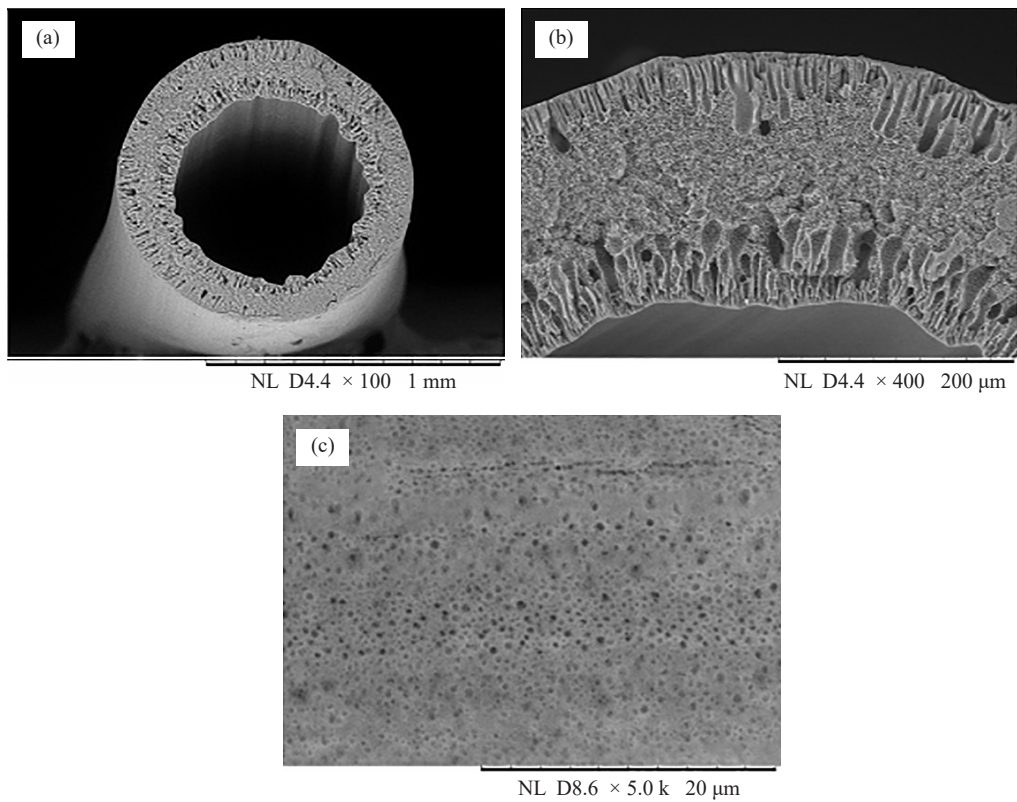


Figure 3. SEM cross-sectional images (a), cross-sectional area (b) and internal surface (c) of the fibers of the PVDF (M1)

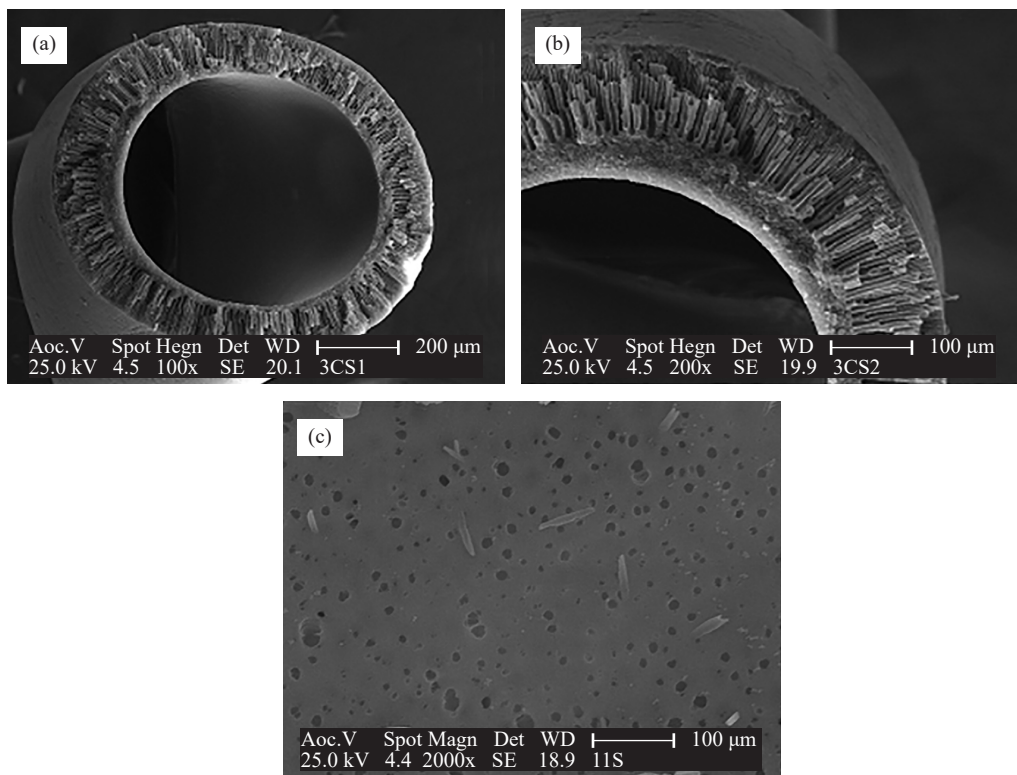


Figure 4. SEM cross-sectional images (a), cross-sectional area (b) and internal surface (c) of the fibers of the PSF (M1)

3.1 Characteristics of membrane

The results of measuring the average pore size, effective porosity, critical pressure input, total porosity and contact angle of the membrane surface with the water of PVDF and PSF membranes are presented in Table 5. In the process of making asymmetric membranes, the overall porosity of the membrane can be controlled using the relative composition of the material in the polymer solution. As shown in Table 5, the porosities of PVDF and PSF membranes are 72.21% and 71.41%, respectively. The high porosity of the membranes produced is due to the low concentration of polymer in the polymer solution. To assess the resistance of the membranes to wetting, a Critical Entry Pressure of water (CEPw) was performed. In the gas-liquid membrane contact, the membrane holes must be filled with gas and prevent the introduction of liquid into the membrane pores. The introduction of absorbent liquid into the membrane pores reduces the contact between the gas and liquid and increases the resistance of the membrane mass transfer. Therefore, the use of high-resistance wetting membranes against wetting is preferred for gas-gas applications in liquid-gas membrane contactor. As can be seen from Table 3, the membrane of the PVDF fiber has a greater CEPw value than the nylon fiber membrane of the PSF. As already mentioned, PVDF polymer is more hydrophobic than PSF polymer. Therefore, further hydrophobicity of the PVDF membrane increases the contact angle with this membrane water and also increases the CEPw of this membrane. Figure 5 shows the penetration of nitrogen gas (N_2) for average pressure values. According to the data of Table 5 and Figure 5, the nitrogen gas permeability in the membrane of the PVDF fiber membrane is higher than the PSF membrane. The higher the gas permeability in this membrane the average pore size of the membrane is larger. The chemical carbon dioxide gas test was carried out using a 1 molar monoethanolamide solution in a gas-liquid membrane contactor. Liquid adsorbent flows in the shell of the module and contact with the skin layer of the membranes, and pure carbon dioxide gas flows in the direction of the membrane cavity in the opposite direction to the liquid flow. The amount of carbon dioxide gas absorption of membranes was measured and compared with the change in the intensity of the adsorbent fluid flow. The results of the experiments on carbon dioxide gas adsorption in terms of fluid flow intensity are shown in Figure 6. Based on Figure 6, the flux absorption of carbon dioxide in both membranes increases with increasing absorption fluid flow due to the reduction in the thickness of the boundary layer of the liquid around the fibers by increasing the liquid velocity, which leads to a decrease in the fluid transfer mass transfer resistance. Also, with increasing fluid velocity, the flow regime changes from relaxed to turbulent, which results in the absorption of more carbon dioxide gas. As shown in Figure 6, in low currents from absorbing fluid, the carbon dioxide gas absorption flux increases both slowly and with gentle gradients, and the liquid flow rate is about $150\text{ (mL}\cdot\text{min}^{-1}\text{)}$ the slope of the gas absorption flux significantly increases, indicating a decrease in the thickness of the boundary layer around the fibers. It is also seen from Figure 6 that the adsorption rate of the PVDF membrane gas is higher than that of the PSF membrane. As seen from the results of the specification of the membrane, the contact angle of the Polyvinylidine Fluoride fiber membrane is greater than the polysulfone membrane, so the penetration of water into the pores of the PSF membrane is easier than the PVDF membrane, and as this membrane is in the early stages of the process absorption gets wet. In this case, the membrane resistance controls the mass transfer process. The wetting of the membrane can increase the total transfer mass resistance and greatly affects the absorption flux⁵⁷⁻⁶¹. Also, the effective porosity of the PVDF membrane surface is much higher than that of the PSF membrane, resulting in a higher level of liquid and gas contact in the membrane than the PSF membrane, which increases the mass transfer rate. At the intrinsic intensity of the adsorbent flow of $300\text{ mL}\cdot\text{min}^{-1}$, the maximum flux of carbon dioxide gas is $8.10 \times 10^{-3}\text{ (mol}\cdot\text{m}^{-2}\cdot\text{s}^{-1}\text{)}$ and $6.50 \times 10^{-3}\text{ (mol}\cdot\text{m}^{-2}\cdot\text{s}^{-1}\text{)}$ to an arrangement was made for the PVDF and PSF naphthenic membrane.

Table 5. Specifications of hollow fiber membranes made of PSF and PVDF

membranes	PSF	PVDF
The average pore size (nm)	13.42	21.18
Effective surface porosity (ε/L_p (10^{-3} m $^{-1}$))	546	1250
Critical pressure of water entry ($\times 10^5$ Pa)	5.50	7.00
Total porosity (%)	71.41	72.21
Membrane braking pressure ($\times 10^5$ Pa)	8.50	9.50
Contact ratio with water	64.32	81.23

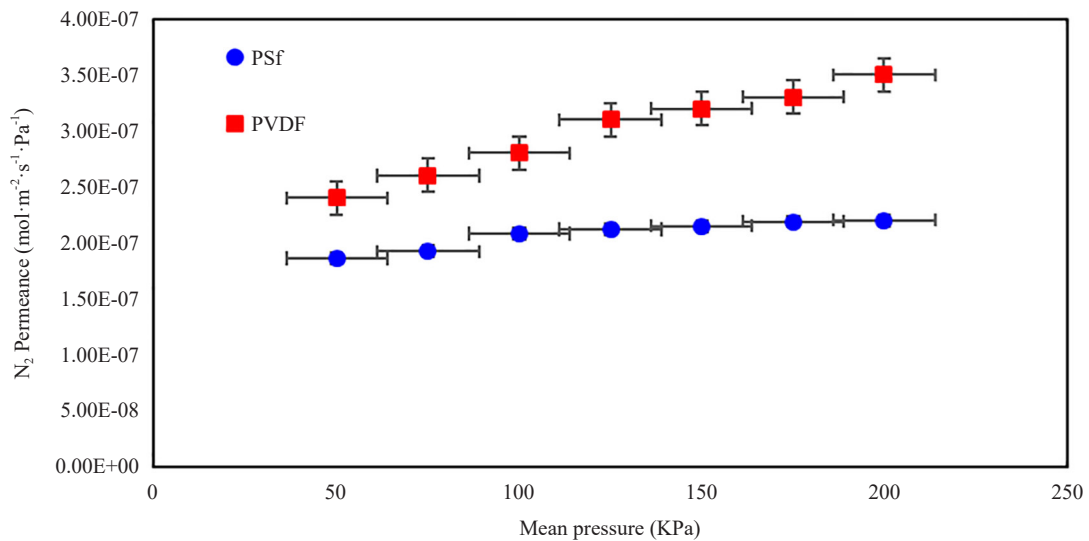


Figure 5. The amount of permeability Absorption of N₂ as a function of the average pressure of the hollow fiber membranes

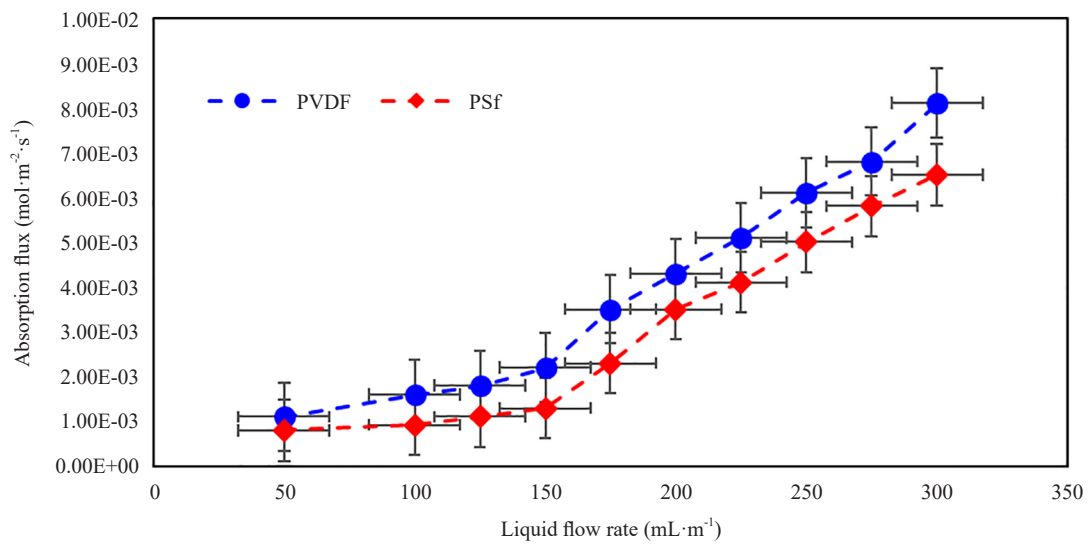


Figure 6. The effect of absorption flow rate (MEA) on the absorption of CO₂ in gas-liquid membrane contactors

3.2 Comparison of long-term carbon dioxide absorption gas hollow fiber membranes

To investigate the applicability of the membrane made in long-term carbon dioxide absorption gas hollow fiber membranes with distilled water, the long-term carbon dioxide absorption gas hollow fiber membranes experiment was carried out for 170 h (approximately 1 week) at ambient temperature, with the results shown in Figure 7. The results of long term CO_2 absorption experiment showed that the CO_2 absorption flux of the PVDF membrane decreased about 76% and reached to 6.88×10^{-3} ($\text{mol}\cdot\text{m}^{-2}\cdot\text{s}^{-1}$), 20 h after the beginning of the process. The CO_2 absorption flux of the PSF membrane decreased by about 24% and reached 9.75×10^{-3} ($\text{mol}\cdot\text{m}^{-2}\cdot\text{s}^{-1}$), 70 h after the beginning of the process. The hollow fiber membrane made with PVDF polymer withstands moisture for up to 20 hours from the start of the process and exhibits an almost constant gas absorption flux, while the membrane made with polysulfide has withstood moisture for 70 hours. These factors make the polysulfone membrane more resistant to the penetration of the adsorbent liquid and therefore have a longer resistance to moisture. Also, the drop in absorption flux of the polysulfone membrane is significantly lower than that of the other membrane, indicating higher resistance to moisture.

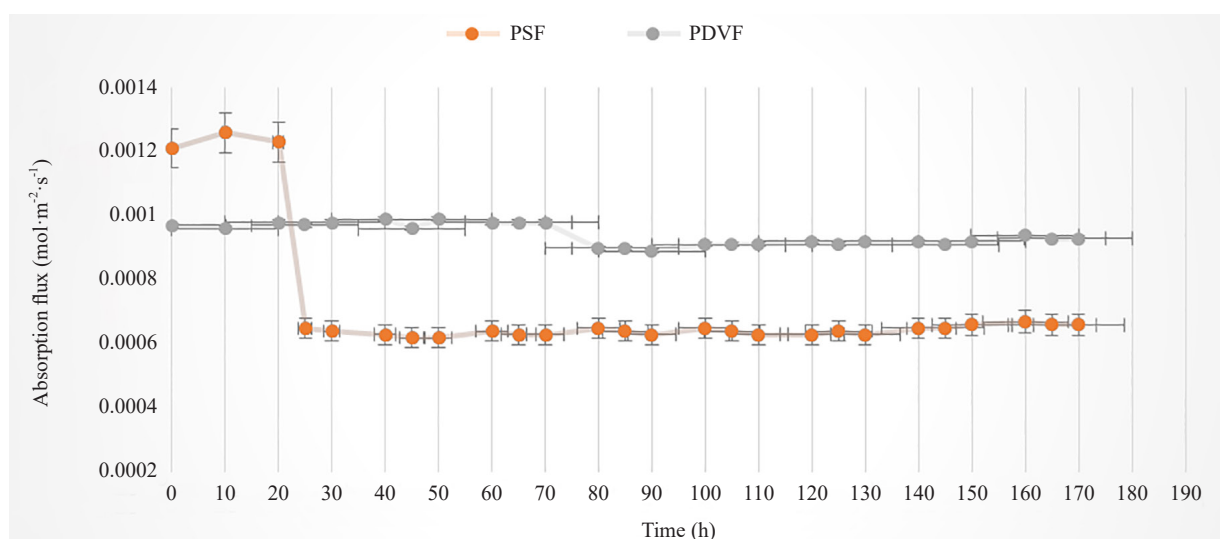


Figure 7. The carbon dioxide absorption flux over time

4. Conclusion

In this study, fiber membranes were fabricated from PVDF and PSF using a wet phase separation method. They were used for chemical absorption of carbon dioxide gas by a $1 \text{ mol}\cdot\text{L}^{-1}$ monoethanolamide solution in the gas-liquid membrane contact system. The results show that the total porosity of the PVDF and PSF membranes is 72.71% and 71.41%, respectively, which is relatively high due to the low concentration of polymer in the polymer solution. The critical entry pressure of water for the water inlet of the PVDF membrane is significantly higher than that of the PSF membrane, which is due to the greater hydrophobicity of the membrane. Nitrogen gas permeability increased for both membranes with increasing gas pressure, and this increase was higher for PVDF membranes. The carbon dioxide gas absorption flux of both membranes increased with increasing absorption liquid velocity. Using a membrane made of poly(vinylidene fluoride) (PVDF), the maximum CO_2 absorption flux was 8.10×10^{-3} ($\text{mol}\cdot\text{m}^{-2}\cdot\text{s}^{-1}$) at a liquid flow rate of $300 \text{ mL}\cdot\text{min}^{-1}$.

Conflict of interest

The author declares no competing financial interest.

References

- [1] Cai, J. J.; Hawboldt, K.; Abedinzadegan Abdi, M. Improving gas absorption efficiency using a novel dual membrane contactor. *J. Membr. Sci.* **2016**, *510*, 249-258.
- [2] Vahidi, M.; Matin, N. S.; Goharrokhi, M.; Jenab, M. H.; Abdi, M. A.; Najibi, S. H. Correlation of CO₂ solubility in N-methyl diethanolamine + piperazine aqueous solutions using extended Debye-Hückel model. *J. Chem. Thermodyn.* **2009**, *41*(11), 1272-1278.
- [3] Cai, J. J.; Hawboldt, K.; Abedinzadegan Abdi, M. Contaminant removal from natural gas using dual hollow fiber membrane contactors. *J. Membr. Sci.* **2012**, *397-398*(15), 9-16.
- [4] Iovane, P.; Nanna, F.; Ding, Y.; Bikson, B.; Molino, A. Experimental test with polymeric membrane for the biogas purification from CO₂ and H₂S. *Fuel* **2014**, *135*, 352-358.
- [5] Faiz, R.; Al-Marzouqi, M. Insights on natural gas purification: Simultaneous absorption of CO₂ and H₂S using membrane contactors. *Sep. Purif. Technol.* **2011**, *76*(3), 351-361.
- [6] Luis, P.; Gerven, T. V.; Bruggen, B. V. D. Recent developments in membrane based technologies for CO₂ capture. *Prog. Energy Combust. Sci.* **2012**, *38*, 419-448.
- [7] George, G.; Bhoria, N.; AlHallaq, S.; Abdala, A.; Mittal, V. Polymer membranes for acid gas removal from natural gas. *Sep. Purif. Technol.* **2016**, *158*, 333-356.
- [8] Rahbari-Sisakht, M.; Ismail, A. F.; Rana, D.; Matsuura, T.; Emadzadeh, D. Effect of SMM concentration on morphology and performance of surface modified PVDF hollow fiber membrane contactor for CO₂ absorption. *Sep. Purif. Technol.* **2013**, *116*(15), 67-72.
- [9] Rahbari-Sisakht, M.; Ismail, A. F.; Rana, D.; Matsuura, T. Carbon dioxide stripping from diethanolamine solution through porous surface modified PVDF hollow fiber membrane contactor. *J. Membr. Sci.* **2013**, *425*, 270-275.
- [10] Bhide, B. D.; Voskericyan, A.; Stern, S. A. Hybrid processes for the removal of acid gases from natural gas. *J. Membr. Sci.* **1998**, *140*(1), 27-49.
- [11] Mansourizadeh, A.; Ismail, A. F. Effect of additives on the structure and performance of polysulfone hollow fiber membranes for CO₂ absorption. *J. Membr. Sci.* **2010**, *348*(1-2), 260-267.
- [12] Bakeri, G.; Ismail, A. F.; Shariaty-Niassar, M. Effect of polymer concentration on the structure and performance of polyetherimide hollow fiber membranes. *J. Membr. Sci.* **2010**, *363*(1-2), 103-111.
- [13] Naimabc, R.; Ismailab, A. F.; Mansourizadehd, A. Preparation of microporous PVDF hollow fiber membrane contactors for CO₂ stripping from diethanolamine solution. *J. Membr. Sci.* **2012**, *392-393*, 29-37.
- [14] Rahbari-Sisakht, M.; Ismail, A. F.; Matsuura, T. Development of asymmetric polysulfone hollow fiber membrane contactor for CO₂ absorption. *Sep. Purif. Technol.* **2012**, *86*, 215-220.
- [15] Rahbari-Sisakht, M.; Ismail, A. F.; Rana, D.; Matsuura, T. Effect of different additives on the physical and chemical CO₂ absorption in polyetherimide hollow fiber membrane contactor system. *Sep. Purif. Technol.* **2012**, *98*, 472-480.
- [16] Mansourizadeh, A.; Ismail, A. F.; Abdullah, M. S.; Ng, B. C. Preparation of polyvinylidene fluoride hollow fiber membranes for CO₂ absorption using phase inversion promoter additives. *J. Membr. Sci.* **2010**, *355*(1-2), 200-207.
- [17] Ismail, A. F.; Dunkin, I. R.; Gallivan, S. L.; Shilton, S. J. Production of super selective polysulfone hollow fiber membranes for gas separation. *Polym.* **1999**, *40*(23), 6499-6506.
- [18] Luis, P.; Van der Bruggen, B.; Van Gerven, T. Non-dispersive absorption for CO₂ capture: From the laboratory to industry. *J. Chem. Technol. Biotechnol.* **2011**, *86*(6), 769-775.
- [19] Rahbari-Sisakht, M.; Ismail, A. F.; Matsuura, T. Effect of bore fluid composition on structure and performance of asymmetric polysulfone hollow fiber membrane contactor for CO₂ absorption. *Sep. Purif. Technol.* **2012**, *88*, 99-106.
- [20] Khaisri, S.; deMontigny, D.; Tontiwachwuthikul, P.; Jiraratananon, R. CO₂ stripping from monoethanolamine using a membrane contactor. *J. Membr. Sci.* **2011**, *376*(1-2), 110-118.
- [21] Li, J. L.; Chen, B. H. Review of CO₂ absorption using chemical solvents in hollow fiber membrane contactors. *Sep. Purif. Technol.* **2005**, *41*(2), 109-122.
- [22] Rangwala, H. A. Absorption of carbon dioxide into aqueous solutions using hollow fiber membrane contactors. *J. Membr. Sci.* **1996**, *112*(2), 229-240.
- [23] Wang, D.; Li, K.; Teo, W. K. Porous PVDF asymmetric hollow fiber membranes prepared with the use of small molecular additives. *J. Membr. Sci.* **2000**, *178*(1-2), 13-23.
- [24] Naim, R.; Ismail, A. F.; Mansourizadeh, A. Preparation of microporous PVDF hollow fiber membrane contactors for CO₂ stripping from diethanolamine solution. *J. Membr. Sci.* **2012**, *392*, 29-37.
- [25] Naim, R.; Ismail, A. F. Effect of polymer concentration on the structure and performance of PEI hollow fiber

membrane contactor for CO₂ stripping. *J. Hazard. Mater.* **2013**, *250-251*, 354-361.

[26] Choi, S. H.; Tasselli, F.; Jansen, J. C.; Barbieri, G.; Drioli, E. Effect of the preparation conditions on the formation of asymmetric poly(vinylidene fluoride) hollow fibre membranes with a dense skin. *Eur. Polym. J.* **2010**, *46*(8), 1713-1725.

[27] Kianfar, E.; Pirouzfar, V.; Sakhaeinia, H. An experimental study on absorption/stripping CO₂ using mono-ethanol amine hollow fiber membrane contactor. *J. Taiwan Inst. Chem. Eng.* **2017**, *80*, 954-962.

[28] Salimi, M.; Pirouzfar, V.; Kianfar, E. Enhanced gas transport properties in silica nanoparticles filler polystyrene nanocomposite membranes. *Colloid Polym. Sci.* **2017**, *295*, 215-226.

[29] Salimi, M.; Pirouzfar, V.; Kianfar, E. Novel nanocomposite membranes prepared with PVC/ABS and silica nanoparticles for C₂H₆/CH₄ separation. *Polym. Sci., Ser. A* **2017**, *59*, 566-574.

[30] Kianfar, E.; Salimi, M.; Kianfar, F.; Kianfar, M.; Razavikia, S. A. CO₂/N₂ separation using polyvinyl chloride isophthalic acid/aluminium nitrate nanocomposite membrane. *Macromol. Res.* **2019**, *27*(1), 83-89.

[31] Ma, H.; Hsiao, B. S.; Chu, B. Functionalized electrospun nanofibrous microfiltration membranes for removal of bacteria and viruses. *J. Membr. Sci.* **2014**, *452*, 446.

[32] Wang, Z.; Yu, H.; Xia, J.; Zhang, F.; Li, F.; Xia, Y.; Li, Y. Novel GO-blended PVDF ultrafiltration membranes. *Desalination* **2012**, *299*, 50-54.

[33] Stamatialis, D. F.; Papenburg, B. J.; Gironés, M.; Saiful, S.; Bettahalli, S. N.; Schmitmeier, S.; Wessling, M. Medical applications of membranes: Drug delivery, artificial organs and tissue engineering. *J. Membr. Sci.* **2008**, *308*(1-2), 1-34.

[34] Dong, G.; Woo, K. T.; Kim, J.; Kim, J. S.; Lee, Y. M. Simulation and feasibility study of using thermally rearranged polymeric hollow fiber membranes for various industrial gas separation applications. *J. Membr. Sci.* **2015**, *496*, 229-241.

[35] Zhang, X.; Chen, Y.; Konsowa, A. H.; Zhu, X.; Crittenden, J. C. Evaluation of an innovative polyvinyl chloride (PVC) ultrafiltration membrane for wastewater treatment. *Sep. Purif. Technol.* **2009**, *70*(1), 71-78.

[36] Wang, C.; Wu, H.; Qu, F.; Liang, H.; Niu, X.; Li, G. Preparation and properties of polyvinyl chloride ultrafiltration membranes blended with functionalized multi-walled carbon nanotubes and MWCNTs/Fe₃O₄ hybrids. *J. Appl. Polym. Sci.* **2016**, *133*(20), 1-8.

[37] Roy, K. J.; Anjali, T. V.; Sujith, A. Asymmetric membranes based on poly(vinyl chloride): Effect of molecular weight of additive and solvent power on the morphology and performance. *J. Mater. Sci.* **2017**, *52*, 5708-5725.

[38] Xu, J.; Xu, Z. L. Poly(vinyl chloride) (PVC) hollow fiber ultrafiltration membranes prepared from PVC/additives/solvent. *J. Membr. Sci.* **2002**, *208*, 203-212.

[39] Teow, Y. H.; Ooi, B. S.; Ahmad, A. L. Fouling behaviours of PVDF-TiO₂ mixed-matrix membrane applied to humic acid treatment. *J. Water Process Eng.* **2017**, *15*, 89-98.

[40] Gao, W.; Liang, H.; Ma, J.; Han, M.; Chen, Z. L.; Han, Z. S.; Li, G. B. Membrane fouling control in ultrafiltration technology for drinking water production: A review. *Desalination* **2011**, *272*(1-3), 1-8.

[41] Sadeghi, M.; Pourafshari Chenar, M.; Rahimian, M.; Moradi, S.; Dehaghani, A. S. Gas permeation properties of polyvinylchloride/polyethyleneglycol blend membranes. *J. Appl. Polym. Sci.* **2008**, *110*(2), 1093-1098.

[42] Behboudi, A.; Jafarzadeh, Y.; Yegani, R. Polyvinyl chloride/polycarbonate blend ultrafiltration membranes for water treatment. *J. Membr. Sci.* **2017**, *534*, 18-24.

[43] Yang, Y. F.; Wan, L. S.; Xu, Z. K. Surface hydrophilization for polypropylene microporous membranes: A facile interfacial crosslinking approach. *J. Membr. Sci.* **2009**, *326*, 372-381.

[44] Rabiee, H.; Shahabadi, S. M.; Mokhtare, A.; Rabiee, H.; Alvandifar, N. Enhancement in permeation and antifouling properties of PVC ultrafiltration membranes with addition of hydrophilic surfactant additives: Tween-20 and Tween-80. *J. Environ. Chem. Eng.* **2006**, *4*(4), 4050-4061.

[45] Fan, X.; Su, Y.; Zhao, X.; Li, Y.; Zhang, R.; Zhao, J.; Jiang, Z.; Zhu, J.; Ma, Y.; Liu, Y. Fabrication of polyvinyl chloride ultrafiltration membranes with stable antifouling property by exploring the pore formation and surface modification capabilities of polyvinyl formal. *J. Membr. Sci.* **2014**, *464*, 100-109.

[46] Ng, L. Y.; Mohammad, A. W.; Leo, C. P.; Hilal, N. Polymeric membranes incorporated with metal/metal oxide nanoparticles: A comprehensive review. *Desalination* **2013**, *308*, 15-33.

[47] Rabiee, H.; Vatanpour, V.; Farahani, M. H.; Zarrabi, H. Improvement in flux and antifouling properties of PVC ultrafiltration membranes by incorporation of zinc oxide (ZnO) nanoparticles. *Sep. Purif. Technol.* **2015**, *156*, 299-310.

[48] Zhang, Y.; Cui, P.; Du, T.; Shan, L.; Wang, Y. Development of a sulfated Y-doped nonstoichiometric zirconia/polysulfone composite membrane for treatment of wastewater containing oil. *Sep. Purif. Technol.* **2009**, *70*(2), 153-159.

[49] Ng, L. Y.; Leo, C. P.; Mohammad, A. W. Optimizing the incorporation of silica nanoparticles in polysulfone/poly(vinyl alcohol) membranes with response surface methodology. *J. Appl. Polym. Sci.* **2011**, *121*, 1804-1814.

[50] Yang, Y.; Zhang, H.; Wang, P.; Zheng, Q.; Li, J. The influence of nano-sized TiO_2 fillers on the morphologies and properties of PSF UF membrane. *J. Membr. Sci.* **2007**, *288*(1-2), 231-238.

[51] Zhao, Y.; Lu, J.; Liu, X.; Wang, Y.; Lin, J.; Peng, N.; Li, J.; Zhao, F. Performance enhancement of polyvinyl chloride ultrafiltration membrane modified with graphene oxide. *J. Colloid Interface Sci.* **2016**, *480*, 1-8.

[52] Dorost, F.; Omidkhah, M. R.; Pedram, M. Z.; Moghadam, F. J. Fabrication and characterization of polysulfone/polyimide-zeolite mixed matrix membrane for gas separation. *Chem. Eng. J.* **2011**, *171*(3), 1469-1476.

[53] Goh, P. S.; Ismail, A. F.; Sanip, S. M.; Ng, B. C.; Aziz, M. Recent advances of inorganic fillers in mixed matrix membrane for gas separation. *Sep. Purif. Technol.* **2011**, *81*(3), 243-264.

[54] Shah, R.; Gale, J. D.; Payne, M. C. Comparing the acidities of zeolites and SAPOs from first principles. *Chem. Commun.* **1997**, *1*, 131-132.

[55] Hoek, E. M.; Ghosh, A. K.; Huang, X.; Liang, M.; Zink, J. I. Physical-chemical properties, separation performance, and fouling resistance of mixed-matrix ultrafiltration membranes. *Desalination* **2011**, *283*, 89-99.

[56] Han, R.; Zhang, S.; Liu, C.; Wang, Y.; Jian, X. Effect of NaA zeolite particle addition on poly(phthalazinone ether sulfone ketone) composite ultrafiltration (UF) membrane performance. *J. Membr. Sci.* **2009**, *345*(1-2), 5-12.

[57] Li, J. F.; Xu, Z. L.; Yang, H.; Yu, L. Y.; Liu, M. Effect of TiO_2 nanoparticles on the surface morphology and performance of microporous PES membrane. *Appl. Surf. Sci.* **2009**, *255*(9), 4725-4732.

[58] Wang, R.; Li, D. F.; Zhou, C.; Liu, M.; Liang, D. T. Impact of DEA solutions with and without CO_2 loading on porous polypropylene membranes intended for use as contactors. *J. Membr. Sci.* **2004**, *229*(1-2), 147-157.

[59] Atchariyawut, S.; Feng, C.; Wang, R. Effect of membrane structure on mass-transfer in the membrane gas-liquid contacting process using microporous PVDF hollow fibers. *J. Membr. Sci.* **2006**, *285*, 272-281.

[60] Khaisri, S.; Demontigny, D. Comparing membrane resistance and absorption performance of three different membranes in a gas absorption membrane contactor. *Sep. Purif. Technol.* **2009**, *65*, 290-297.

[61] Rajabzadeh, S.; Yoshimoto, S.; Teramoto, M.; Al-Marzouqi, M.; Matsuyama, H. CO_2 absorption by using PVDF hollow fiber membrane contactors with various membrane structures. *Sep. Purif. Technol.* **2009**, *69*(2), 210-220.

[62] Marzouk, S. A.; Al-Marzouqi, M. H.; Abdullatif, N.; Ismail, Z. M. Removal of percentile level of H_2S from pressurized $\text{H}_2\text{S}-\text{CH}_4$ gas mixture using hollow fiber membrane contactors and absorption solvents. *J. Membr. Sci.* **2010**, *360*(1-2), 436-441.

[63] Lv, Y.; Yu, X.; Tu, S. T.; Yan, J.; Dahlquist, E. Experimental studies on simultaneous removal of CO_2 and SO_2 in a polypropylene hollow fiber membrane contactor. *Appl. Energy* **2012**, *97*, 283-288.

[64] Ghasem, N.; Al-Marzouqi, M.; Rahim, N. A. Preparation and properties of polyethersulfone hollow fiber membranes with o-xylene as an additive used in membrane contactors for CO_2 absorption. *Sep. Purif. Technol.* **2012**, *99*, 91-103.

[65] Rajabzadeh, S.; Yoshimoto, S.; Teramoto, M.; Al-Marzouqi, M.; Ohmukai, Y.; Maruyama, T.; Matsuyama, H. Effect of membrane structure on gas absorption performance and long-term stability of membrane contactors. *Sep. Purif. Technol.* **2013**, *108*, 65-73.

[66] Sadoogh, M.; Mansourizadeh, A.; Mohammadinik, H. An experimental study on the stability of PVDF hollow fiber membrane contactors for CO_2 absorption with alkanolamine solutions. *RSC Adv.* **2015**, *5*, 86031-86040.